

# Channel Models, Favorable Propagation and Multi-Stage Linear Detection in Cell-Free Massive MIMO

Roya Gholami  
EURECOM

Communication Systems Department  
Sophia Antipolis, France  
Email: roya.gholami@eurecom.fr

Laura Cottatellucci  
Friedrich-Alexander University  
Institute for Digital Communications  
Erlangen, Germany  
Email: laura.cottatellucci@fau.de

Dirk Slock  
EURECOM  
Communication Systems Department  
Sophia Antipolis, France  
Email: dirk.slock@eurecom.fr

**Abstract**—We consider a cell-free MIMO system in uplink, comprising a massive number of distributed transmit and receive antennas. In our distributed antenna system (DAS), transmit and receive antennas are distributed according to homogeneous point processes (PP) and the received signals are processed jointly at a central processing unit (CPU). In centralized massive MIMO systems, the phenomenon of *favorable propagation* has been observed: when the number of receive antennas tends to infinity while the number of transmit antennas remains finite, the users' channels become almost orthogonal and low complexity detection via matched filtering is almost optimal. We analyze the properties of DASs in asymptotic conditions when the network dimensions go to infinity with given intensities of the transmit and receive antenna PPs. We study the analytical conditions of favorable propagation in DASs with two kinds of channels, namely, channels with path loss and transmit and receive antennas in line of sight (LoS) or in multipath Rayleigh fading. We show that the analytical conditions of favorable propagation are satisfied for channels impaired by path loss and Rayleigh fading while they do not hold in the case of LoS channels, motivating the use and analysis of multi-stage receivers. Simulation results of the favorable propagation conditions and the performance of multi-stage detectors for finite systems validate the asymptotic analytical results.

## I. INTRODUCTION

Distributed antenna systems (DAS) are expected to play a fundamental role in next generation wireless systems. In DASs, access points (AP) are distributed over a wide area and connected to a centralized processing unit. They present great potentials to enhance spectral and power efficiency compared to traditional cellular systems with centralized base stations (BS). DASs have been extensively studied in downlink, see, e.g., [1], [2] and references therein. Fundamental limits of DASs in uplink have been studied in [3]–[5]. The capacity per unit area of DASs in uplink has been analyzed in [4], [5] leveraging on a mathematical framework based on Euclidean random matrices and assuming that the network dimensions tend to infinity. To reap the benefits promised by this analysis completely, the use of a centralized optimal joint processing is crucial. However, an optimal maximum likelihood detector has an unaffordable complexity for large systems. Interestingly, in centralized MIMO systems, the high complexity of centralized joint detectors has been successfully addressed by massive MIMO systems [6]. In massive MIMO systems, as the number of antennas at the BS increases and the number of users remains constant, the channels between users and BS tend to become jointly orthogonal determining a phenomenon known as *favorable propagation* [7]. Under orthogonality conditions low complexity matched filters are optimum and matched filters attain the same performance of maximum likelihood

detectors, asymptotically. To leverage simultaneously on the advantages of DASs and massive MIMO systems, the concept of cell-free (CF) massive MIMO was introduced in [8], [9]. A CF massive MIMO system consists of a massive number of geographically distributed single-antenna access points (APs), which jointly serve a much smaller number of users. If favorable propagation held, matched filtering could be again utilized as a low complexity and almost-optimal detection method.

In massive MIMO systems with centralized BSs, the assumption of Rayleigh fading provides realistic guidelines for system design. However, in DASs where the APs are massively distributed and several of them could be very close to users and in direct line of sight (LoS), it becomes relevant to investigate the effects of LoS and path loss on the property of favorable propagation. An initial numerical analysis for CF massive MIMO in Rayleigh fading was presented in [10]. In [11], we studied favorable propagation conditions for 1-dimensional (1D) CF massive MIMO networks with APs and users in LoS. Conditions for favorable propagation were expressed in terms of eigenvalue moments of the channel covariance matrix. In this paper, we extend the analysis to 2-dimensional (2D) DASs and consider the two extreme cases of DASs with all antennas in LoS or in non-LoS and Rayleigh fading and we study analytically their properties. We model APs and users as two independent uniform PPs over a regular grid. Under this assumption, the inclusion of path loss and LoS or Rayleigh fading leads to classes of random matrices similar to the Euclidean random matrices proposed in [4], [5]. We show analytically that the favorable propagation conditions are not satisfied in CF massive MIMO systems with APs and users in LoS. On the contrary, they hold in the case of path loss plus multipath Rayleigh fading. When matched filtering is not almost optimum, the use of low complexity linear multiuser detection becomes very appealing in practical systems. Then, by extending the unified analytical framework proposed in [12], we analyze the performance of both polynomial expansion detectors in [13] and multi-stage Wiener filters in [14] and show their equivalence in large scale DAS. Their performance analysis confirms the expectations of the favorable propagation analysis and the substantial benefits of these detectors compared to matched filters when the favorable propagation conditions are not satisfied.

The remainder of this paper is organized as follows. Section

II introduces the system and channel model. The eigenvalue moments of the covariance matrix of channel with path loss with transmit and receive antennas in LoS or with Rayleigh fading are presented in Section III. In Section IV, we analyze the analytical conditions of favorable propagation for the two kinds of channels and the performance of multi-stage detectors. Numerical results are illustrated in Section V. Finally, concluding remarks are summarized in Section VI.

*Notation:* Throughout the paper,  $\mathbf{i} = \sqrt{-1}$ , the superscript  $T$ ,  $*$ , and  $H$  denote the transpose, conjugate, and conjugate transpose operator, respectively. Uppercase and lowercase bold symbols are utilized to denote matrices and vectors, respectively. The expectation and the Euclidean norm operators are denoted by  $\mathbb{E}(\cdot)$  and  $\|\cdot\|$ , respectively.  $\text{tr}(\cdot)$  and  $\text{diag}(\cdot)$  denote the trace and the square diagonal matrix whose diagonal elements are given by the elements of the vector argument, respectively. The Kronecker operator is denoted by  $\otimes$ . Finally,  $\mathcal{CN}(\nu, \sigma^2)$  denotes a complex Gaussian distribution with mean  $\nu$  and variance  $\sigma^2$ .

## II. SYSTEM MODELS

We consider a DAS in uplink with users and APs equipped with a single antenna and independently and uniformly distributed over a squared box of side  $L$  and area  $A = L^2$  in  $\mathbb{R}^2$ , denoted by  $\mathcal{A}_L = [-\frac{L}{2}, +\frac{L}{2}] \times [-\frac{L}{2}, +\frac{L}{2}]$ . For the sake of analytical tractability, we assume that users and APs are located on a grid in  $\mathcal{A}_L$ . Let  $\tau > 0$  be an arbitrary small real such that  $L = \theta\tau$  with  $\theta$  positive, even integer. Let  $\mathbf{w} = ((-\theta + 2w_x)\tau/2, (-\theta + 2w_y)\tau/2)$  with  $w_x, w_y \in \mathbb{Z}$ , we denote by  $\mathcal{A}_L^\#$  the set of points regularly spaced in  $\mathcal{A}_L$  by  $\tau$ , i.e.,  $\mathcal{A}_L^\# \equiv \{\mathbf{w} | \mathbf{w} \in \mathcal{A}_L, w_x, w_y = 0, 1, \dots, \theta - 1\}$ . We model the distributed users and APs as homogeneous PPs  $\Phi_T$  and  $\Phi_R$  in  $\mathcal{A}_L^\#$  characterized by parameters  $\beta_T = \rho_T\tau^2$  and  $\beta_R = \rho_R\tau^2$ , where  $\rho_T$  and  $\rho_R$  are the intensities, i.e., the number per unit area, of users and APs, respectively. Then,  $N_T = \rho_T L^2 = \beta_T \theta^2$  and  $N_R = \rho_R L^2 = \beta_R \theta^2$  are the number of users and APs, respectively.

All the APs are connected to a central processing unit via a back-haul network such that detection is performed jointly. Users transmit at the same power  $P$ . At the central processing unit, the discrete time  $N_R$ -dimensional received signal vector is given by

$$\mathbf{y} = \sqrt{P}\mathbf{G}\mathbf{x} + \mathbf{n}, \quad (1)$$

where  $\mathbf{x}$  is the  $N_T$ -dimensional column vector of independent and identically distributed (i.i.d.) transmitted symbols with  $\mathbb{E}\{|x_j|^2\} = 1$ ;  $\mathbf{G}$  is the  $N_R \times N_T$  matrix of channel coefficients whose  $(i, j)$ -element  $g_{ij} = g(\mathbf{r}_i, \mathbf{t}_j)$  denotes the channel coefficient between transmitter  $j$  and receiver  $i$  with Euclidean coordinates  $\mathbf{t}_j = (t_{x,j}, t_{y,j})$  and  $\mathbf{r}_i = (r_{x,i}, r_{y,i})$ , respectively. The  $N_R$ -dimensional vector  $\mathbf{n}$  denotes the complex additive white Gaussian noise vector with i.i.d. components having zero mean and variance  $\sigma^2$ .

In order to define the channel coefficients, we introduce the path loss matrix  $\hat{\mathbf{G}}$  with  $(i, j)$  element given by

$$\hat{g}_{ij} = \hat{g}(\mathbf{r}_i, \mathbf{t}_j) = \begin{cases} \frac{d_0^\alpha}{\|\mathbf{r}_i - \mathbf{t}_j\|_2^\alpha} & \text{if } \|\mathbf{r}_i - \mathbf{t}_j\|_2 > d_0 \\ 1 & \text{otherwise,} \end{cases} \quad (2)$$

where  $d_0$  is a reference distance and  $2\alpha$  is the path loss exponent. At short distances between APs and users, i.e., for  $\|\mathbf{r}_i - \mathbf{t}_j\|_2 \leq d_0$ , the loss is assumed to be negligible and  $\hat{g}_{ij} = 1$  in order to remove model artifacts. In the case of antennas in LoS, the channel coefficients impaired by path loss are given by  $g_{ij} = g(\mathbf{r}_i, \mathbf{t}_j) = \hat{g}(\mathbf{r}_i, \mathbf{t}_j)\exp(-i2\pi\lambda^{-1}\|\mathbf{r}_i - \mathbf{t}_j\|_2)$ , being  $\lambda$  the radio signal wavelength. In the case of non-LoS channels with Rayleigh fading, they are given by  $g_{ij} = \hat{g}(\mathbf{r}_i, \mathbf{t}_j)h_{ij}$ , where  $h_{i,j} \sim \mathcal{CN}(0, 1)$  are i.i.d. complex Gaussian variables modeling small scale fading.

## III. MATHEMATICAL RESULTS FOR DAS ANALYSIS

In this section we derive a tight approximation of the eigenvalue moments of the channel covariance matrix  $\mathbf{C} = \mathbf{G}^H\mathbf{G}$  that can be efficiently applied to the analysis of favorable propagation properties in CF massive MIMO and the design and analysis of multi-stage linear detectors.

The eigenvalue moments or, shortly, the moments of the channel covariance matrix  $\mathbf{C}$  are defined as follows

$$m_{\mathbf{C}}^{(n)} = \int \mu^n dF_{\mathbf{C}}(\mu) = \frac{1}{N_T} \mathbb{E}\{\text{tr}(\mathbf{C}^n)\} \quad n \in \mathbb{N} \quad (3)$$

where  $\mu$  and  $F_{\mathbf{C}}(\mu)$  denote the eigenvalue and empirical eigenvalue distribution of matrix  $\mathbf{C}$ , respectively.

Following the approach in [4], [5], [15], we decompose the path loss matrix,  $\hat{\mathbf{G}}$ , as follows

$$\hat{\mathbf{G}} = \Psi_R \hat{\mathbf{T}} \Psi_T^H \quad (4)$$

where  $\hat{\mathbf{T}}$  is a  $\theta^2 \times \theta^2$  matrix depending only on the function  $\hat{g}(\mathbf{r}_i, \mathbf{t}_j)$ ,  $\Psi_R$  and  $\Psi_T$  are  $N_R \times \theta^2$  and  $N_T \times \theta^2$  random matrices depending only on random APs' and users' locations, respectively. In order to define the matrices  $\Psi_T$ ,  $\Psi_R$ , and  $\hat{\mathbf{T}}$ , we consider the  $\theta^2 \times \theta^2$  path loss matrix  $\hat{\mathbf{G}}$  of a system with  $\theta^2$  transmit and receive antennas regularly spaced in  $\mathcal{A}_L^\#$ . It can be shown [16] that  $\hat{\mathbf{G}}$  is a symmetric block Toeplitz matrix of  $\theta \times \theta$  Toeplitz blocks and, asymptotically, for  $\theta^2 \rightarrow \infty$ , it admits an eigenvalue decomposition based on a  $\theta^2 \times \theta^2$  2D discrete Fourier transform<sup>1</sup> (DFT) matrix  $\mathbf{F}$  [17]. Then, we consider the decomposition  $\hat{\mathbf{G}} = \mathbf{F}\hat{\mathbf{T}}\mathbf{F}^H$ , where the matrix  $\hat{\mathbf{T}}$  is a deterministic, asymptotically diagonal matrix whose diagonal elements are the discrete Fourier series of the first row of  $\hat{\mathbf{G}}$ . The random matrices  $\Psi_R$  and  $\Psi_T$  are obtained by extracting independently and uniformly at random  $N_R$  and  $N_T$  rows of matrix  $\mathbf{F}$ .

In the following subsections, we obtain the eigenvalue moments of the channel covariance matrices for the two channel models considered in this paper.

<sup>1</sup>The 1D DFT matrix over  $N$  points is the  $N \times N$  matrix with element in row  $i$  and column  $j$  given by  $(\mathbf{F}_1)_{ij} = \frac{1}{\sqrt{N}}e^{-2\pi i(i-1)(j-1)/N}$ . The definition can be extended to 2D and the 2D DFT matrix is given by  $\mathbf{F} = \mathbf{F}_1 \otimes \mathbf{F}_1$ .

### A. Eigenvalue Moments for Antennas in LoS

In this section we derive the eigenvalue moments for DASs with transmitters and receivers in LoS and channel attenuation given by path loss. We extend the results for 1D-DASs presented in [11] to 2D-DASs. The derivation follows the same lines as in [11]. The matrix  $\mathbf{G}$  for transmitters and receivers in LoS admits a decomposition similar to  $\tilde{\mathbf{G}}$ , i.e.,  $\mathbf{G} = \Psi_R \mathbf{T} \Psi_T^H$ . As in [5], [15], the eigenvalue moments of the channel covariance matrix are obtained by approximating the random matrices  $\Psi_R$  and  $\Psi_T$  by the independent matrices  $\Phi_R$  and  $\Phi_T$ , respectively, consisting of i.i.d. zero mean complex Gaussian elements with variance  $\theta^{-2}$  to obtain matrix  $\tilde{\mathbf{G}} = \Phi_R \mathbf{T} \Phi_T^H$ . The derivation of the eigenvalue moments follows the techniques proposed in [12], [18]. The results for 2D-DASs extend the ones for 1D-DASs proposed in [11] and are summarized in the following proposition.

**PROPOSITION 1** *Let  $g(\mathbf{r}_i, \mathbf{t}_j)$  be the function of channel coefficients in LoS,  $T(f_1, f_2)$  with  $(f_1, f_2) \in [-1/2, +1/2]^2$  be the 2D Fourier series of the sequence obtained by sampling  $g(\mathbf{r}_i, \mathbf{t}_j)$  over the regular grid  $\mathcal{A}_\infty^\#$ , and  $m_{\mathbf{T}}^{(2\ell)} = \int_{-1/2}^{+1/2} \int_{-1/2}^{+1/2} |T(f_1, f_2)|^{2\ell} df_1 df_2$ . Consider the matrix  $\tilde{\mathbf{C}} = \tilde{\mathbf{G}}^H \tilde{\mathbf{G}}$  with  $\tilde{\mathbf{G}} = \Phi_R \mathbf{T} \Phi_T^H$ . For  $\theta^2, N_R, N_T \rightarrow +\infty$  with  $N_T/\theta^2 \rightarrow \beta_T$  and  $N_R/\theta^2 \rightarrow \beta_R$ ,  $\tilde{C}_{kk}^{(\ell)}$ , the  $k$ -th diagonal element of matrix  $\tilde{\mathbf{C}}^\ell$  and  $m_{\tilde{\mathbf{C}}}^{(\ell)}$ , the eigenvalue moment of order  $\ell$  of the matrix  $\tilde{\mathbf{C}}$  converge to a deterministic value given by*

$$\tilde{C}_{kk}^{(\ell)} = m_{\tilde{\mathbf{C}}}^{(\ell)} = \sum_{n=0}^{\ell-1} \sigma^{(\ell-n)} m_{\tilde{\mathbf{C}}}^{(n)} \quad \text{for any } k \text{ and } \ell \geq 2$$

with

$$\sigma^{(\ell)} = \int \int \mathbb{P}^{(\ell)}(|T(f_1, f_2)|^2) df_1 df_2$$

and  $\mathbb{P}^{(\ell)}(|T(f_1, f_2)|^2)$  polynomial in  $|T(f_1, f_2)|^2$  recursively given by

$$\begin{aligned} \mathbb{P}^{(\ell)}(|T(f_1, f_2)|^2) &= \beta_T m_{\tilde{\mathbf{C}}}^{(\ell-1)} |T(f_1, f_2)|^2 + \\ &+ \beta_R \beta_T |T(f_1, f_2)|^2 \sum_{s=0}^{\ell-2} m_{\tilde{\mathbf{C}}}^{(s)} \mathbb{P}^{(\ell-s-1)}(|T(f_1, f_2)|^2) \\ &+ \beta_T^2 |T(f_1, f_2)|^2 \sum_{s=0}^{\ell-2} \sum_{r=1}^{\ell-2-s} m_{\tilde{\mathbf{C}}}^{(s)} m_{\tilde{\mathbf{C}}}^{(r)} \mathbb{P}^{(\ell-s-r-1)}(|T(f_1, f_2)|^2). \end{aligned}$$

The initial values of the recursion are  $\tilde{C}_{kk}^{(0)} = m_{\tilde{\mathbf{C}}}^{(0)} = 1$ ,  $\mathbb{P}^{(1)}(|T(f_1, f_2)|^2) = \beta_R |T(f_1, f_2)|^2$  and  $\tilde{C}_{kk}^{(1)} = m_{\tilde{\mathbf{C}}}^{(1)} = \sigma^{(1)} = \beta_R m_{\tilde{\mathbf{T}}}^{(2)}$ .

Proposition 1 suggests a simple algorithm to determine  $m_{\tilde{\mathbf{C}}}^{(\ell)}$  and  $\tilde{C}_{kk}^{(\ell)}$  detailed in the following.

#### Algorithm

Initial step: Let  $\mu_0 = \rho_0(x) = 1$ ,  $\sigma^{(1)} = \mu_1 = \beta_R m_{\tilde{\mathbf{T}}}^{(2)}$ ,  $\rho_1(x) = \beta_R x$ , and  $\ell = 2$ .

Step  $\ell$ : • Define polynomial in  $x$   $\rho_\ell(x) = \beta_T \mu_{\ell-1} x + \beta_R \beta_T x \sum_{s=0}^{\ell-2} \mu_s \rho_{\ell-s-1}(x) +$

$\beta_T^2 x \sum_{s=0}^{\ell-2} \sum_{r=1}^{\ell-2-s} \mu_s \mu_r \rho_{\ell-s-r-1}(x)$  and write it as a polynomial in  $x$ .

- In  $\rho_\ell(x)$ , replace the monomial  $x, x^2, \dots, x^\ell$  by the moments  $m_{\tilde{\mathbf{T}}}^{(2)}, m_{\tilde{\mathbf{T}}}^{(4)}, \dots, m_{\tilde{\mathbf{T}}}^{(2\ell)}$ , respectively and assign the result to  $\sigma^{(\ell)}$ .
- Compute  $\mu_\ell = \sum_{n=0}^{\ell-1} \sigma^{(\ell-n)} \mu_n$ .
- Assign  $\mu_\ell$  to  $m_{\tilde{\mathbf{C}}}^{(\ell)}$  and  $\tilde{C}_{kk}^{(\ell)}$ .
- Increase  $\ell$  by a unit.

By applying the previous algorithm we obtain the following eigenvalue moments.

$$m_{\tilde{\mathbf{C}}}^{(1)} = \beta_R m_{\tilde{\mathbf{T}}}^{(2)}, \quad (5)$$

$$m_{\tilde{\mathbf{C}}}^{(2)} = \beta_R^2 \beta_T m_{\tilde{\mathbf{T}}}^{(4)} + \beta_R (\beta_R + \beta_T) (m_{\tilde{\mathbf{T}}}^{(2)})^2, \quad (6)$$

$$\begin{aligned} m_{\tilde{\mathbf{C}}}^{(3)} &= \beta_R^3 \beta_T^2 m_{\tilde{\mathbf{T}}}^{(6)} + 3\beta_R^2 \beta_T (\beta_R + \beta_T) m_{\tilde{\mathbf{T}}}^{(2)} m_{\tilde{\mathbf{T}}}^{(4)} \\ &+ [\beta_R \beta_T (3\beta_R + \beta_T) + \beta_R^3] (m_{\tilde{\mathbf{T}}}^{(2)})^3. \end{aligned} \quad (7)$$

### B. Eigenvalue Moments for Rayleigh Fading Channels

In this subsection, we consider the channel matrix for Rayleigh fading given by  $\mathbf{G} = (\hat{g}_{ij} h_{ij})_{i=1, \dots, N_R}^{j=1, \dots, N_T}$  and we determine an asymptotic approximation of its eigenvalue moments by approximating  $\mathbf{G}$ , the path loss matrix, by  $\tilde{\mathbf{G}} = (\check{g}_{ij})_{i=1, \dots, N_R}^{j=1, \dots, N_T} = \Phi_R \hat{\mathbf{T}} \Phi_T^H$ . Then, the following result holds.

**PROPOSITION 2** *Let  $\hat{g}(\mathbf{r}_i, \mathbf{t}_j)$  be the path loss function,  $\hat{T}(f_1, f_2)$ , with  $(f_1, f_2) \in [-1/2, 1/2]^2$ , be the 2D discrete Fourier series of the sequence obtained by sampling  $\hat{g}(\mathbf{r}_i, \mathbf{t}_j)$  over a regularly spaced grid  $\mathcal{A}_\infty^\#$ , and  $m_{\hat{\mathbf{T}}}^{(2\ell)} = \int_{-1/2}^{+1/2} \int_{-1/2}^{+1/2} |\hat{T}(f_1, f_2)|^{2\ell} df_1 df_2$ . Consider the matrix  $\tilde{\mathbf{G}} = (\check{g}_{ij} h_{ij})_{i=1, \dots, N_R}^{j=1, \dots, N_T}$ . As  $L \rightarrow +\infty$ , the eigenvalue moment of order  $\ell$  of the matrix  $\tilde{\mathbf{C}} = \tilde{\mathbf{G}}^H \tilde{\mathbf{G}}$  converges to the deterministic value given by*

$$m_{\tilde{\mathbf{C}}}^{(\ell)} = (m_{\hat{\mathbf{T}}}^{(2)})^\ell \sum_{k=0}^{\ell-1} \frac{1}{k+1} \binom{\ell-1}{k} \binom{\ell}{k} \beta_T^k \beta_R^{\ell-k} \quad (8)$$

*Sketch of the proof:* The  $\ell$ -th eigenvalue moment of matrix  $\tilde{\mathbf{C}}$  is given by

$$\begin{aligned} m_{\tilde{\mathbf{C}}}^{(\ell)} &= \mathbb{E} \left\{ \frac{1}{N_T} \text{tr}(\tilde{\mathbf{C}}^\ell) \right\} \\ &= \frac{1}{N_T} \sum_{j_1, \dots, j_\ell=1}^{N_T} \sum_{i_1, \dots, i_\ell=1}^{N_R} \mathbb{E} \left\{ \check{g}_{i_1, j_1}^* h_{i_1, j_1}^* \dots \check{g}_{i_\ell, j_\ell}^* h_{i_\ell, j_\ell}^* \check{g}_{i_\ell, j_\ell} h_{i_\ell, j_\ell} \right\} \\ &= \frac{1}{N_T} \sum_{j_1, \dots, j_\ell=1}^{N_T} \sum_{i_1, \dots, i_\ell=1}^{N_R} \mathbb{E} \left\{ h_{i_1, j_1}^* h_{i_1, j_2} \dots h_{i_\ell, j_\ell}^* h_{i_\ell, j_1} \right\} \\ &\quad \times \mathbb{E} \left\{ \check{g}_{i_1, j_1}^* \check{g}_{i_1, j_2} \dots \check{g}_{i_\ell, j_\ell}^* \check{g}_{i_\ell, j_1} \right\} \end{aligned} \quad (9)$$

where the last equality stems from the statistical independence of  $\check{g}_{i,j}$  and  $h_{i,j}$ . It is possible to show that for  $L \rightarrow +\infty$ , non vanishing contributions to the eigenvalue moments in (9) are given by terms with indices  $(j_1, i_1, j_2, i_2, \dots, j_\ell, i_\ell)$  satisfying the non-crossing partition condition [19]. Then, a closed-form expression of the eigenvalue moments is found by resorting to techniques of non-crossing partitions widely utilized in

random matrix theory to derive eigenvalue moments. Given the sequence of  $(j_1, i_1, j_2, i_2, \dots, j_\ell, i_\ell)$ , we consider the two sets of indices eventually repeated  $\mathcal{J} = \{j_1, j_2, \dots, j_\ell\}$  and  $\mathcal{I} = \{i_1, i_2, \dots, i_\ell\}$  and denote by  $p_1$  and  $p_2$  the number of distinct indices in  $\mathcal{J}$  and  $\mathcal{I}$ . Additionally, we associate to the sequence a bipartite graph with directed edges from one to the other set given by each consecutive pair of indices in the sequence. A sequence is a non-crossing partition if

- 1)  $p_1 + p_2 = \ell + 1$ ;
- 2) Whenever an edge from  $\mathcal{J}$  to  $\mathcal{I}$  appears in the bipartite graph, then it should also appear in the opposite direction from  $\mathcal{I}$  and  $\mathcal{J}$ ,
- 3) The bipartite graph is a tree.

Consider the sets obtained from  $\mathcal{J}$  and  $\mathcal{I}$  by removing repetitions of indices. It is possible to show that the number of distinct non-crossing partitions for the resulting sets is given by [20]

$$\frac{1}{p_1} \binom{\ell-1}{p_1-1} \binom{\ell}{p_1-1} = \frac{1}{\ell-p_2+1} \binom{\ell-1}{\ell-p_2} \binom{\ell}{p_1-1} \quad (10)$$

Additionally, choosing the indices of  $\mathcal{J}$  and  $\mathcal{I}$  from the sets  $\{1, \dots, N_R\}$  and  $\{1, \dots, N_T\}$  respectively, there are

$$N_T(N_T-1)\dots(N_T-p_1-1)N_R(N_R-1)\dots(N_R-p_2-1) = \mathcal{O}(N_T^{p_1} N_R^{p_2}) \quad (11)$$

possible choices of indices yielding similar bipartite graphs. Then, in total, there are  $N_T^{p_1} N_R^{p_2} \frac{1}{p_1} \binom{\ell-1}{p_1-1} \binom{\ell}{p_1-1}$  sequences of indices satisfying the non-crossing partition conditions with  $p_1$  vertices in  $\{1, \dots, N_T\}$  and  $\ell+1-p_1$  vertices in  $\{1, \dots, N_R\}$ .

Let us observe that the expectation of each term corresponding to a non-crossing partition with  $p_1$  vertices in  $\{1, \dots, N_T\}$  and  $\ell+1-p_2$  vertices in  $\{1, \dots, N_R\}$ , gives the same contribution. In particular,

$$\mathbb{E}\{h_{i_1, j_1}^* h_{i_1, j_2} \dots h_{i_\ell, j_\ell}^* h_{i_\ell, j_1}\} = 1 \quad (12)$$

since in the expectation appear  $\ell$  independent factors  $|h_{i,j}|^2$  with  $h_{i,j} \sim \mathcal{CN}(0, 1)$ . Additionally,

$$\mathbb{E}\{\check{g}_{i_1, j_1}^* \check{g}_{i_1, j_2} \dots \check{g}_{i_\ell, j_\ell}^* \check{g}_{i_\ell, j_1}\} = \frac{(m_{\tilde{\mathbf{T}}})^\ell}{\theta^{2\ell}} \quad (13)$$

since in the expectations appear  $\ell$  independent factors  $|\check{g}_{i,j}|^2$  and  $\mathbb{E}\{|\check{g}_{i,j}|^2\} = \frac{1}{\theta^2} m_{\tilde{\mathbf{T}}}^{(2)}$  where  $m_{\tilde{\mathbf{T}}}^{(2)}$  denotes the eigenvalue moment of the diagonal matrix  $\tilde{\mathbf{T}}\tilde{\mathbf{T}}^H$ . Note that as  $\theta^2 \rightarrow +\infty$ ,  $m_{\tilde{\mathbf{T}}}^{(2)}$  coincides with the moment defined in the statement of Proposition 2. From (10), (11), (12), and (13) we obtain

$$m_{\tilde{\mathbf{C}}}^{(\ell)} = \frac{1}{N_T} \sum_{p_1=1}^{\ell} \frac{1}{p_1} \binom{\ell-1}{p_1-1} \binom{\ell}{p_1-1} N_R^{\ell+1-p_1} N_T^{p_1} \left(\frac{m_{\tilde{\mathbf{T}}}}{\theta^2}\right)^\ell$$

that leads to (8). This concludes our proof.

The first three eigenvalue moments of the covariance matrix for the Rayleigh fading channel converge to the following values

$$m_{\tilde{\mathbf{C}}}^{(1)} = \beta_R m_{\tilde{\mathbf{T}}}^{(2)}, \quad (14)$$

$$m_{\tilde{\mathbf{C}}}^{(2)} = \beta_R(\beta_R + \beta_T)(m_{\tilde{\mathbf{T}}}^{(2)})^2, \quad (15)$$

$$m_{\tilde{\mathbf{C}}}^{(3)} = [\beta_R \beta_T (3\beta_R + \beta_T) + \beta_R^3](m_{\tilde{\mathbf{T}}}^{(2)})^3. \quad (16)$$

#### IV. PROPERTIES AND PERFORMANCE ANALYSIS

In this section, we analyze the favorable propagation conditions for LoS and Rayleigh fading channel in DASs through the characteristics of their channel eigenvalue moments. In a favorable propagation environment, when the users have almost orthogonal channels, the channel covariance matrix  $\mathbf{R}$  is almost diagonal and satisfies the following properties

$$\frac{m_{\mathbf{R}}^{(\ell)}}{\text{tr}[(\text{diag}(\mathbf{R}))^\ell]} \approx 1 \quad \forall \ell \in \mathbb{N}^+ \quad (17)$$

where  $m_{\mathbf{R}}^{(\ell)}$  denotes the  $\ell$ -order eigenvalue moment of matrix  $\mathbf{R}$ . These properties are asymptotically satisfied for centralized massive MIMO systems, in rich scattering environments, when the number of users stays finite while the number of antennas at the central base station tends to infinity.

By making use of the observation that in large DAS, as  $L \rightarrow \infty$ ,  $\tilde{C}_{kk} = \beta_R m_{\tilde{\mathbf{T}}}^{(2)}$ , we obtain that  $\text{tr}[(\text{diag}(\tilde{\mathbf{C}}))^\ell] = \beta_R^\ell (m_{\tilde{\mathbf{T}}}^{(2)})^\ell$  such that (17) specializes for DAS with LoS channel and  $\ell = 2, 3$  as follows

$$\frac{m_{\tilde{\mathbf{C}}}^{(2)}}{\beta_R^2 (m_{\tilde{\mathbf{T}}}^{(2)})^2} = 1 + \frac{\beta_T}{\beta_R} + \beta_T \frac{m_{\tilde{\mathbf{T}}}^{(4)}}{(m_{\tilde{\mathbf{T}}}^{(2)})^2} \quad (18)$$

$$\begin{aligned} \frac{m_{\tilde{\mathbf{C}}}^{(3)}}{\beta_R^3 (m_{\tilde{\mathbf{T}}}^{(2)})^3} &= 1 + 3\frac{\beta_T}{\beta_R} + \frac{\beta_T^2}{\beta_R^2} + 3\beta_T \left(1 + \frac{\beta_T}{\beta_R}\right) \frac{m_{\tilde{\mathbf{T}}}^{(4)}}{(m_{\tilde{\mathbf{T}}}^{(2)})^2} + \\ &+ \beta_T^2 \frac{m_{\tilde{\mathbf{T}}}^{(6)}}{(m_{\tilde{\mathbf{T}}}^{(2)})^3} \end{aligned} \quad (19)$$

As  $\beta_R \rightarrow \infty$  while  $\beta_T$  is kept constant, i.e., for  $\beta_T/\beta_R \rightarrow 0$  and  $\beta_T > 0$ , the ratios (18) and (19) converge to the following limiting values

$$\begin{aligned} \frac{m_{\tilde{\mathbf{C}}}^{(2)}}{\beta_R^2 (m_{\tilde{\mathbf{T}}}^{(2)})^2} &\rightarrow 1 + \beta_T \frac{m_{\tilde{\mathbf{T}}}^{(4)}}{(m_{\tilde{\mathbf{T}}}^{(2)})^2} \\ \frac{m_{\tilde{\mathbf{C}}}^{(3)}}{\beta_R^3 (m_{\tilde{\mathbf{T}}}^{(2)})^3} &\rightarrow 1 + 3\beta_T \frac{m_{\tilde{\mathbf{T}}}^{(4)}}{(m_{\tilde{\mathbf{T}}}^{(2)})^2} + \beta_T^2 \frac{m_{\tilde{\mathbf{T}}}^{(6)}}{(m_{\tilde{\mathbf{T}}}^{(2)})^3} \end{aligned} \quad (20)$$

and conditions (17) are not satisfied. For DASs with path loss and Rayleigh fading channel, the moment ratios in (17) converge to one for all  $\ell \geq 1$ , as  $\beta_T/\beta_R \rightarrow 0$  and  $\beta_R \rightarrow \infty$  as shown in the following

$$\begin{aligned} \frac{m_{\tilde{\mathbf{C}}}^{(\ell)}}{\text{tr}[(\text{diag}(\tilde{\mathbf{C}}))^\ell]} &= \frac{\beta_R^\ell (m_{\tilde{\mathbf{T}}}^{(2)})^\ell \sum_{k=0}^{\ell-1} \frac{1}{k+1} \binom{\ell-1}{k} \binom{\ell}{k} \left(\frac{\beta_T}{\beta_R}\right)^k}{\beta_R^\ell (m_{\tilde{\mathbf{T}}}^{(2)})^\ell} \\ &= 1 + \sum_{k=1}^{\ell-1} \frac{1}{k+1} \binom{\ell-1}{k} \binom{\ell}{k} \left(\frac{\beta_T}{\beta_R}\right)^k \rightarrow 1 \end{aligned} \quad (21)$$

Then, conditions (17) are satisfied and Rayleigh fading channel offers favorable propagation. Systems with favorable propagation can efficiently utilize low complexity matched filters at the central processing unit since this filter achieves almost optimal performance in such environments. However, when conditions (17) are not satisfied, even linear multiuser detectors are expected to provide substantial gains compared to the matched filter. In the following, we consider low complexity multi-stage detectors including both polynomial expansion detectors, e.g., [13], and multi-stage Wiener filters

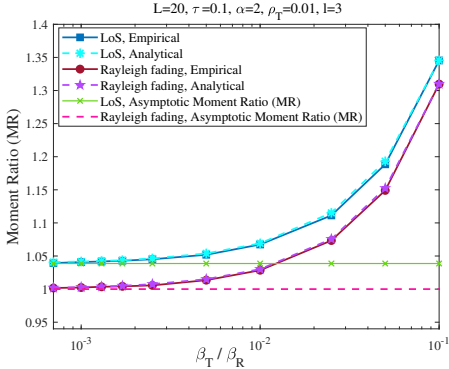


Fig. 1. Favorable propagation conditions  $MR = m_{\tilde{\mathbf{C}}}^{(\ell)} / \text{tr}[(\text{diag}(\tilde{\mathbf{C}}))^\ell]$  versus  $\beta_T / \beta_R$ .

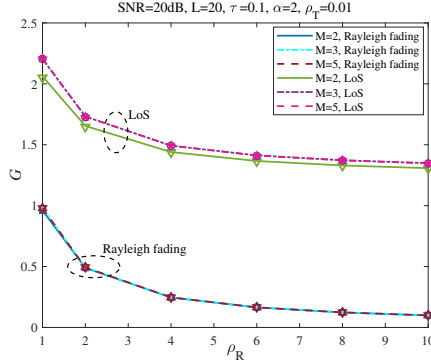


Fig. 2. Asymptotic (solid lines) and empirical (markers) gains  $G$  versus  $\rho_R$  for multi-stage detectors ( $M = 2, 3, 5$ ), with path loss plus LoS or plus Rayleigh fading.

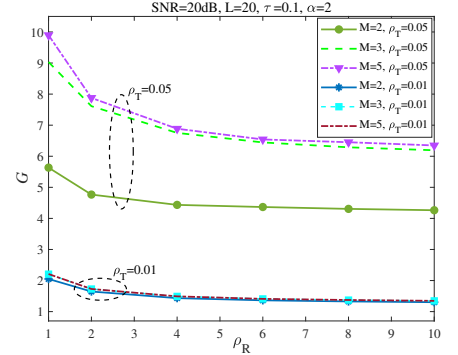


Fig. 3. Gain  $G$  versus  $\rho_R$  of multi-stage detectors ( $M = 2, 3, 5$ ) for path loss plus LoS channels and  $\rho_T \in \{0.01, 0.05\}$ .

[14] and we analyze their performance in terms of their signal to interference and noise ratio (SINR) by applying the unified framework proposed in [12], [21]. In [12], it is shown that both design and analysis of multi-stage detectors with  $M$  stages can be described by a matrix  $\mathbf{S}(X)$  defined as

$$\mathbf{S}(X) = \begin{pmatrix} X^{(2)} + \sigma^2 X^{(1)} & \cdots & X^{(M+1)} + \sigma^2 X^{(M)} \\ X^{(3)} + \sigma^2 X^{(2)} & \cdots & X^{(M+2)} + \sigma^2 X^{(M+1)} \\ \vdots & \ddots & \vdots \\ X^{(M+1)} + \sigma^2 X^{(M)} & \cdots & X^{(2M)} + \sigma^2 X^{(2M-1)} \end{pmatrix}$$

and a vector  $\mathbf{s}(X) = (X^{(1)}, X^{(2)}, \dots, X^{(M)})^T$  where  $X = m_{\tilde{\mathbf{C}}}$  for polynomial expansion detectors and  $X = \tilde{C}_{kk}$  for multi-stage Wiener filters. From the asymptotic property that  $\tilde{C}_{kk}^{(\ell)} = m_{\tilde{\mathbf{C}}}^{(\ell)}$  for any  $k$  and  $\ell$ , we can conclude that multi-stage Wiener filters and polynomial expansion detectors are equivalent in DAS. Additionally, the performance of a centralized processor implementing an  $M$ -stage detector is given by [12]

$$\text{SINR}_M = \frac{\mathbf{s}^T(m_{\tilde{\mathbf{C}}})\mathbf{S}^{-1}(m_{\tilde{\mathbf{C}}})\mathbf{s}(m_{\tilde{\mathbf{C}}})}{1 - \mathbf{s}^T(m_{\tilde{\mathbf{C}}})\mathbf{S}^{-1}(m_{\tilde{\mathbf{C}}})\mathbf{s}(m_{\tilde{\mathbf{C}}})} \quad (22)$$

For  $M = 1$ , a multi-stage detector reduces to a matched filter and (22) can be applied to determine its performance and  $\text{SINR}_1$  yields the SINR at the output of a matched filter.

## V. NUMERICAL RESULTS

In this section, we validate the analytical asymptotic results by simulations and analyze the performance of multi-stage detectors in large scale systems. Throughout this section, we consider the following scenario. The channel is characterized by  $\alpha = 2$  and reference distance  $d_0 = 1$ . The transmit antennas are distributed according to a homogeneous PP with intensity  $\rho_T = 0.01$  over a finite network of area  $A = L^2 = 400$  while the intensity of the receivers varies in the range  $\rho_R = [0.1, 15]$  in Fig.1 and  $\rho_R = [1, 10]$  in Fig. 2 and Fig.3. Fig.1 shows the moment ratio  $m_{\tilde{\mathbf{C}}}^{(\ell)} / \text{tr}[(\text{diag}(\tilde{\mathbf{C}}))^\ell]$  versus  $\beta_T / \beta_R = \rho_T / \rho_R$  for  $\ell = 3$ . The x-axis is plotted in logarithmic scale. The analytical moment ratios match almost perfectly the ratios for the simulated finite systems. As predicted analytically, the favorable propagation conditions are not satisfied for LoS channel while they hold in the case of the Rayleigh fading. For small ratios  $\beta_T / \beta_R$ , the curves of LoS and Rayleigh fading converge to the asymptotic moment ratios in (20) and (21), respectively. In Fig. 2 and Fig.3, we consider a system with average signal to noise ratio (SNR) at the transmitters equal

to 20dB and analyze the gain of a multi-stage Wiener filter or equivalently a polynomial expansion detector over a matched filter in terms of the its normalized increase in SINR defined as follows

$$G = \frac{\text{SINR}_M - \text{SINR}_1}{\text{SINR}_1}.$$

Fig. 2 compares the performance of the two channel models and presents gain  $G$  versus  $\rho_R$ , the intensity of receivers for  $M$ -stage Wiener filters with  $M = 2, 3, 5$ . The analytical results in solid lines are obtained under the asymptotic assumption  $L \rightarrow \infty$ . The empirical results shown by markers are obtained for  $L = 20$  and averaging over 100 network realizations. Simulations show an excellent match between the asymptotic performance and empirical results. In the case of Rayleigh fading, as favorable propagation conditions are satisfied, the performance gap between matched filter and multi-stage detectors tends to vanish and gain  $G$  becomes negligible as  $\rho_R$  increases while  $\rho_T$  is kept constant. Then, for  $\rho_R$  sufficiently large, the matched filter achieves almost optimal performance. On the contrary, in the LoS case, the performance gap between the matched filter and multi-stage detectors is dramatic with an increase in SINR of about 140% even for systems with 1000 receive antennas per transmitter per unit area. It is interesting to note that for the considered channel models, this dramatic performance enhancement can be attained already with a very simple 2-stage detector and higher complexity multi-stage detectors offer only incremental improvements at least at very low system loads. In Fig. 3 we analyze the effect of  $\rho_T / \rho_R$ , the system load per unit area, in the case of transmit and receive antennas in LoS. Fig. 3 shows gain  $G$  for  $\rho_T = 0.05$  and  $\rho_T = 0.01$  as the intensity of receivers varies. Increasing the system load, the SINR increase offered by a 2-stage detector increases enormously and for higher load, also the increments offered by higher order multi-stage detectors over a 2-stage detector become significant.

## VI. CONCLUSION

In this paper, we considered a DAS in uplink. We showed analytically that the favorable propagation conditions are not satisfied in CF massive MIMO system with transmit and receive antennas in LoS. On the contrary, they hold in the case of Rayleigh fading. Then, we analyzed the performance of multi-stage detectors in these two scenarios and showed the relevance of their use especially in systems with antennas in LoS.

## REFERENCES

- [1] Y. Lin and W. Yu, "Downlink spectral efficiency of distributed antenna systems under a stochastic model," *IEEE Transactions on Wireless Communications*, vol. 13, no. 12, pp. 6891–6902, 2014.
- [2] J. Li, D. Wang, P. Zhu, J. Wang, and X. You, "Downlink spectral efficiency of distributed massive MIMO systems with linear beamforming under pilot contamination," *IEEE Transactions on Vehicular Technology*, vol. 67, no. 2, pp. 1130–1145, 2017.
- [3] L. Dai, "A comparative study on uplink sum capacity with co-located and distributed antennas," *IEEE Journal on Selected Areas in Communications*, vol. 29, no. 6, pp. 1200–1213, 2011.
- [4] L. Cottatellucci, "Spectral efficiency of extended networks with randomly distributed transmitters and receivers," in *2014 IEEE China Summit & International Conference on Signal and Information Processing (ChinaSIP)*. IEEE, 2014, pp. 673–677.
- [5] —, "Capacity per unit area of distributed antenna systems with centralized processing," in *2014 IEEE Global Communications Conference*. IEEE, 2014, pp. 1746–1752.
- [6] T. L. Marzetta, "Noncooperative cellular wireless with unlimited numbers of base station antennas," *IEEE Transactions on Wireless Communications*, vol. 9, no. 11, pp. 3590–3600, Nov. 2010.
- [7] H. Q. Ngo, E. G. Larsson, and T. L. Marzetta, "Aspects of favorable propagation in massive MIMO," in *2014 22nd European Signal Processing Conference (EUSIPCO)*. IEEE, 2014, pp. 76–80.
- [8] H. Q. Ngo, A. Ashikhmin, H. Yang, E. G. Larsson, and T. L. Marzetta, "Cell-free massive MIMO: uniformly great service for everyone," in *2015 IEEE 16th international workshop on signal processing advances in wireless communications (SPAWC)*. IEEE, 2015, pp. 201–205.
- [9] —, "Cell-free massive MIMO versus small cells," *IEEE Transactions on Wireless Communications*, vol. 16, no. 3, pp. 1834–1850, 2017.
- [10] Z. Chen and E. Björnson, "Channel hardening and favorable propagation in cell-free massive MIMO with stochastic geometry," *IEEE Transactions on Communications*, vol. 66, no. 11, pp. 5205–5219, 2018.
- [11] R. Gholami, L. Cottatellucci, and D. Slock, "Favorable propagation and linear multiuser detection for distributed antenna systems," in *ICASSP 2020-2020 IEEE International Conference on Acoustics, Speech and Signal Processing (ICASSP)*. IEEE, 2020, pp. 5190–5194.
- [12] L. Cottatellucci and R. R. Müller, "A systematic approach to multistage detectors in multipath fading channels," *IEEE Transactions on Information Theory*, vol. 51, no. 9, pp. 3146–3158, 2005.
- [13] S. Moshavi, "Multi-user detection for DS-CDMA communications," *IEEE Communications Magazine*, vol. 34, no. 10, pp. 124–136, Oct. 1996.
- [14] J. S. Goldstein, I. S. Reed, and L. L. Scharf, "A multistage representation of the Wiener filter based on orthogonal projections," *IEEE Transactions on Information Theory*, vol. 44, no. 7, Nov. 1998.
- [15] S. Skipetrov and A. Goetschy, "Eigenvalue distributions of large Euclidean random matrices for waves in random media," *arXiv preprint arXiv:1007.1379*, 2010.
- [16] A. Nyberg, "The Laplacian spectra of random geometric graphs," Ph.D. dissertation, 2014.
- [17] R. M. Gray *et al.*, "Toeplitz and circulant matrices: A review," *Foundations and Trends® in Communications and Information Theory*, vol. 2, no. 3, pp. 155–239, 2006.
- [18] L. Cottatellucci, R. R. Müller, and M. Debbah, "Asynchronous CDMA systems with random spreading—Part II: design criteria," *IEEE Transactions on Information Theory*, vol. 56, no. 4, pp. 1498–1520, 2010.
- [19] R. Speicher, "Free probability theory and non-crossing partitions," *Sém. Lothar. Combin.*, vol. 39, p. 38, 1997.
- [20] Z. Bai and J. W. Silverstein, *Spectral analysis of large dimensional random matrices*. Springer, 2010, vol. 20.
- [21] L. Cottatellucci and R. R. Müller, "CDMA systems with correlated spatial diversity: A generalized resource pooling result," *IEEE Transactions on Information Theory*, vol. 53, no. 3, pp. 1116–1136, Mar. 2007.